Available online at www.sciencedirect.com
ScienceDirect
International Journal of Heat and Mass Transfer 51 (2008) 3044–3051
International Journal of HEAT and MASS TRANSFER
www.elsevier.com/locate/ijhmt

Linear stability analysis of a fluid-saturated porous layer subjected to time-dependent heating

Joung Sook Hong [a], Min Chan Kim [b,*], Do-Young Yoon [c], Bum-Jin Chung [d], Sin Kim [d]

[a] Department of Chemical and Biological Engineering, Korea University, Seoul 136-705, Republic of Korea
[b] Department of Chemical Engineering, Cheju National University, Cheju 690-756, Republic of Korea
[c] Department of Chemical Engineering, Kwangwoon University, Seoul 139-701, Republic of Korea
[d] Department of Nuclear and Energy Engineering, Cheju National University, Cheju 690-756, Republic of Korea

Received 15 January 2007; received in revised form 10 September 2007
Available online 5 November 2007

Abstract

A theoretical analysis of thermal instability driven by buoyancy forces under the transient temperature fields is conducted in an initially quiescent, fluid-saturated and horizontal porous layer. Darcy's law is used to explain the characteristics of fluid motion and under the principle of exchange of stabilities, the linear stability theory is employed to derive stability equations. The stability equations are analyzed by the initial value approach with the proper initial conditions. Two stability limits, τ_s and τ_r are obtained under the strong and the relative stability concepts. The critical condition of onset of buoyancy-driven convection is governed by the Darcy–Rayleigh number, as expected. The growth period for disturbances to grow is seemed to be required until the instabilities are detected experimentally. The convective motion can be detected experimentally from a certain time $\tau_0 \cong 4\tau_r$.

Keywords: Buoyancy-driven instability; Porous media; Time-dependent heating; Linear stability theory; Strong stability; Relative stability

1. Introduction

It is well known that the buoyancy-driven phenomena in the porous media have a wide variety of engineering applications, such as geothermal reservoirs, agricultural product storage systems, packed-bed catalytic reactors, the pollutant transport in underground and the heat removal of nuclear power plants. Recently, the buoyancy-driven phenomena in porous media have been extensively studied in connection with the enhanced carbon dioxide dissolution into the saline water confined within the geologically stable formations [1–3].

For the system under the stationary boundary conditions Horton and Rogers [4] and Lapwood [5] conducted the theoretical analysis on the critical condition of the onset of buoyancy-driven motion in fluid-saturated horizontal porous layers. They employed Darcy's law to express the flow characteristics in the porous layers and analyzed the effect of Darcy number on the onset condition of buoyancy-driven convection. However, when the boundary conditions are suddenly changed, as is the case of a temperature step function increase, the basic temperature profile of pure conduction becomes time-dependent and a new problem arises. In this case buoyancy-driven convection sets in before the basic temperature profile becomes fully developed. Most of engineering applications in this field involve developing the nonlinear basic temperature profile. Therefore it is important to predict when the buoyancy-driven motion sets in. To analyze this kind of thermal instability in fluid layers Foster [6] treated the time dependency as an initial value problem. By employing the amplification theory Kaviany [7] analyzed the onset condi-

* Corresponding author. Tel.: +82 64 754 3685; fax: +82 64 755 3670.
E-mail address: mckim@cheju.ac.kr (M.C. Kim).

0017-9310/$ - see front matter © 2007 Elsevier Ltd. All rights reserved.
doi:10.1016/j.ijheatmasstransfer.2007.09.009

Nomenclature

a	dimensionless wave number
a^*	modified wave number, $a\sqrt{\tau}$
c	specific heat (J kg^{-1} K^{-1})
d	fluid layer thickness (m)
Da	Darcy number, K/d^2
E	average thermal energy
g	gravitational acceleration (m s^{-2})
K	permeability (m^2)
k	thermal conductivity (W m^{-1} K^{-1})
P	pressure (Pa)
Ra_γ	Rayleigh number, $\varepsilon g\beta\gamma d^5/(\alpha_e^2\nu)(\rho c)_f/(\rho c)^*$
Ra_D	Darcy–Rayleigh number, $DaRa_\gamma$
Ra_D^*	modified Darcy–Rayleigh number, $Ra_D\tau^{3/2}$
T	temperature (K)
(U, V, W)	velocities in Cartesian coordinates (m s^{-1})
(u, v, w)	dimensionless velocity disturbances in Cartesian coordinates
(X, Y, Z)	Cartesian coordinates (m)
(x, y, z)	dimensionless Cartesian coordinates

Greek symbols

α	thermal diffusivity (m^2 s^{-1})
β	thermal expansion coefficient (K^{-1})
ΔT	temperature difference (K)
Δ_T	thermal penetration depth
δ_T	dimensionless thermal penetration depth
ε	porosity
ζ	dimensionless similarity variable, $z/\tau^{1/2}$
θ_1	dimensionless temperature disturbance, $g\beta d^3 T_1/(\alpha\nu)$
θ_0	dimensionless basic temperature, $\alpha_e(T_0 - T_i)/(\phi d^2)$
μ	viscosity (Pa s)
ρ	density (kg m^{-3})
ν	kinematic viscosity (m^2 s^{-1})
τ	dimensionless time

Subscripts

0	basic quantities
1	perturbation quantities
c	critical conditions
e	effective properties
f	fluid properties
i	initial state
s	solid matrix properties

Superscript

*	quantities in (τ, ζ)-domian

tion of buoyancy-driven convection in the porous medium with internal heat sources. Homsy [8] and Wankat and Homsy [9] introduced the energy method, which suggested necessary stability condition. Caltagirone [10] extended the energy method and the amplification theory to the porous media heated form below. Kim et al. [11] analyzed the onset of Rayleigh–Bénard convection by employing the propagation theory which employs the thermal penetration depth as a length scaling factor and transforms the linearized equations into the similar forms. Later, Kim et al. [12] applied propagation theory to the buoyancy-driven convection in the porous media. Tan and Thorpe [13] proposed maximum-Rayleigh number criterion wherein the temperature profile assumed to be linear within $Z = Z_{max}(t)$, and defined the onset time when newly defined transient-Rayleigh number reached the conventional steady-state Rayleigh number. Recently, Tan et al. [14] extended maximum-Rayleigh number criterion to the porous media.

In the present study thermal instability of initially quiescent, fluid-saturated, horizontal porous layer subjected to time-dependent heating is analyzed theoretically with initial value problem approach. Since the present predictions will be compared with the extant experimental data, the present study may complement the recent theoretical work [1,3] in the onset of buoyancy-driven convection where their predictions have not been justified experimentally.

2. Theoretical analysis

2.1. Governing equations

The system considered here is an initially quiescent, fluid-saturated, horizontal porous layer of depth d, as shown in Fig. 1. The solid substrate has a constant porosity ε and permeability K. And the interstitial fluid is characterized by thermal expansion coefficient β, density ρ, heat capacity $(\rho c)_f$ and kinematic viscosity ν. The porous medium is regarded as a homogeneous and isotropic fluid with heat capacity $(\rho c)_e = \varepsilon(\rho c)_f + (1-\varepsilon)(\rho c)_s$ and thermal conductivity $k_e = \varepsilon k_f + (1-\varepsilon)k_s$. Before heating the fluid layer is maintained at uniform temperature T_i for time $t < 0$. For time $t \geqslant 0$ the lower boundary is heated with constant heating rate γ. For this system the governing equations of

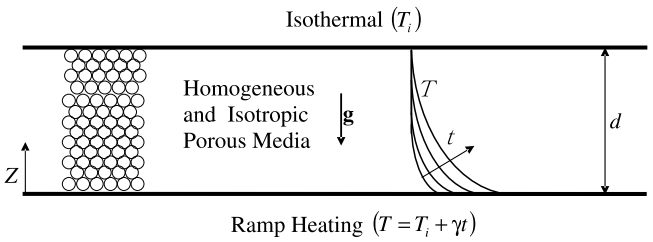

Fig. 1. Schematic diagram of system considered here.

flow and temperature fields are expressed employing the Boussinesq approximation and Darcy's model [15]

$$\nabla \cdot \mathbf{U} = 0, \tag{1}$$

$$\frac{\mu}{K}\mathbf{U} = -\nabla P + \rho \mathbf{g}, \tag{2}$$

$$\left(\frac{\partial}{\partial t} + \varepsilon \frac{(\rho c)_{\mathrm{f}}}{(\rho c)_{\mathrm{e}}}\mathbf{U}\cdot\nabla\right) T = \alpha_{\mathrm{e}}\nabla^2 T, \tag{3}$$

$$\rho = \rho_{\mathrm{i}}[1 - \beta(T - T_{\mathrm{i}})], \tag{4}$$

where $\mathbf{U}$ is the velocity vector, T the temperature, P the pressure, μ the viscosity, $\alpha_{\mathrm{e}}(=k_{\mathrm{e}}/(\rho c)_{\mathrm{e}})$ the effective thermal diffusivity and g the gravitational acceleration. The subscript i represents the initial state. Katto and Masuoka [15] discussed the physical properties of porous medium and showed experimentally the effect of the Darcy number on the critical condition of the onset of buoyancy-driven convection.

The important parameters to describe the present system are the Darcy number Da, the Rayleigh number based on the temporal heating rate Ra_γ and the Darcy–Rayleigh number Ra_{D} defined by

$$Da = \frac{K}{d^2}, \quad Ra_\gamma = \frac{g\beta\gamma d^5}{\alpha_{\mathrm{e}}^2 \nu}\varepsilon\frac{(\rho c)_{\mathrm{f}}}{(\rho c)_{\mathrm{e}}}, \text{ and } Ra_{\mathrm{D}} = DaRa_\gamma, \tag{5}$$

where Ra_γ is rescaled with the temperature scale of $\gamma\, d^2/\alpha_{\mathrm{e}}$. For a system of large Ra_γ, the stability problem becomes transient and very difficult, and the critical time t_{c} to mark the onset of buoyancy-driven motion remains unsolved. For this transient stability analysis we define a set of non-dimensionalized variables τ, z, θ_0 by using the scale of time d^2/α_{e}, length d and temperature $\gamma d^2/\alpha_{\mathrm{e}}$. Then the basic conduction state is represented in dimensionless form by

$$\frac{\partial\theta_0}{\partial\tau} = \frac{\partial^2\theta_0}{\partial z^2} \tag{6}$$

with the following initial and boundary conditions,

$$\theta_0 = 0 \text{ at } \tau = 0, \tag{7a}$$

$$\theta_0 = \tau \text{ at } z = 0 \text{ and } \theta_0 = 0 \text{ at } z = 1. \tag{7b}$$

The above equations can be solved by using the conventional separation of variables technique and Laplace transform method as follows:

$$\theta_0 = \tau(1-z) - 2\sum_{n=0}^{\infty}\frac{\sin(n\pi z)}{(n\pi)^3}\{1 - \exp(-n^2\pi^2\tau)\}, \tag{8a}$$

$$\theta_0 = 4\tau\sum_{n=0}^{\infty}(-1)^n\left[i^2\mathrm{erfc}\left(\frac{n}{\sqrt{\tau}} + \frac{\zeta}{2}\right) + i^2\mathrm{erfc}\left(\frac{n+1}{\sqrt{\tau}} - \frac{\zeta}{2}\right)\right], \tag{8b}$$

where $\zeta = z/\sqrt{\tau}$ and $i^2\mathrm{erfc}(\xi) = \frac{1}{4}\left\{(1+2\xi^2)\mathrm{erfc}(\xi) - \frac{2\xi}{\sqrt{\pi}}\exp(-\xi^2)\right\}$. For the limiting case of $\tau \to 0$, the above two basic temperature fields are well-approximated by

$$\theta_0^*(\zeta) = 4i^2\mathrm{erfc}\left(\frac{\zeta}{2}\right), \tag{9}$$

where $\theta_0^*(\zeta) = \theta_0(\tau,\zeta)/\tau$.

2.2. Stability analysis

Under the linear stability theory the disturbances caused by the onset of thermal convection can be formulated, in dimensionless form, in term of the temperature component θ_1 and the vertical velocity component w_1 by decomposing Eqs. (1)–(4)

$$\nabla^2 w_1 = -\nabla_1^2\theta_1, \tag{10}$$

$$\frac{\partial\theta_1}{\partial\tau} + Ra_{\mathrm{D}} w_1\frac{\partial\theta_0}{\partial z} = \nabla^2\theta_1, \tag{11}$$

where $\nabla^2 = \frac{\partial^2}{\partial x^2} + \frac{\partial^2}{\partial y^2} + \frac{\partial^2}{\partial z^2}$ and $\nabla_1^2 = \frac{\partial^2}{\partial x^2} + \frac{\partial^2}{\partial y^2}$. The velocity component has the scale of α/d and the temperature component has the scale of $\alpha\nu/(g\beta d^3)$. The proper boundary conditions are given by

$$w_1 = \theta_1 = 0 \text{ at } z = 0 \text{ and } z = 1. \tag{12}$$

The boundary conditions represent no flow through the boundaries and the fixed temperature on the upper boundary and the adiabatic conditions of the lower boundary.

According to the normal mode analysis, convective motion is assumed to exhibit the horizontal periodicity [16]. Then the perturbed quantities can be expressed as follows:

$$[w_1(\tau,x,y,z), \theta_1(\tau,x,y,z)] = [w_1(\tau,z), \theta_1(\tau,z)]\exp\lfloor j(a_x x + a_y y)\rfloor, \tag{13}$$

where j is the imaginary number. Substituting the above Eq. (13) into Eqs. (10)–(12) produces the usual amplitude functions in terms of the horizontal wave number $a = (a_x^2 + a_y^2)^{1/2}$.

$$(D^2 - a^2)w_1 = a^2\theta_1, \tag{14}$$

$$\frac{\partial\theta_1}{\partial\tau} = (D^2 - a^2)\theta_1 - Ra_{\mathrm{D}} w_1 D\theta_0, \tag{15}$$

where $D = \mathrm{d}/\mathrm{d}z$.

By employing the Galerkin method, the w_1 and θ_1 are represented by a system of linearly independent functions as

$$w_1 = \sum_{l=1}^{N} A_l(\tau)\sin(l\pi z), \quad \theta_1 = \sum_{l=1}^{N} B_l(\tau)\sin(l\pi z). \tag{16}$$

Here, we choose the trial functions that satisfy the boundary conditions of Eq. (12) for the Darcy equation rather than those for the conventional Navier–Stokes equation. By substituting the above relation into Eqs. (14) and (15) and using the orthogonality of the trial functions, we can obtain a system of N differential equations for the unknown Fourier coefficients $B_l(\tau)$ with N algebraic equations for the relations between unknown coefficients $A_l(\tau)$ and $B_l(\tau)$ as

$$\{(l\pi)^2 + a^2\}A_l = a^2 B_l, \tag{17}$$

$$\frac{\mathrm{d}B_l}{\mathrm{d}\tau} = -\{(l\pi)^2 + a^2\}B_l - 2Ra_{\mathrm{D}}\sum_{m=1}^{N} I_{ml}A_m, \tag{18}$$

where

$$I_{ml} = \int_0^1 \frac{\partial \theta_0}{\partial z} \sin(m\pi z)\sin(l\pi z)\mathrm{d}z = \frac{1}{2\pi^2}\left[\frac{(1-\exp(-(m-l)^2\pi^2\tau))}{(m-l)^2} - \frac{(1-\exp(-(m+l)^2\pi^2\tau))}{(m+l)^2}\right]. \quad (19)$$

Eliminating A_l we get

$$\frac{\mathrm{d}B_l}{\mathrm{d}\tau} = -\{(l\pi)^2 + a^2\}B_l - 2Ra_{\mathrm{D}}\sum_{m=1}^{N} I_{ml}\frac{a^2}{(a^2+(l\pi)^2)}B_m. \quad (20)$$

The system of differential equations of Eq. (20) is solved by the Runge–Kutta fourth- or fifth-order method. To analyze the stability limits by solving Eq. (20), the proper initial conditions are necessary. The most common initial condition is the white noise condition where all spatial frequencies are present and all Fourier coefficients are set to unity. This white noise condition is known as the fastest growing disturbance [6].

In this linear stability analysis, a choice must be made for the criterion for instability. Under the strong stability criterion, the strong stability limit τ_{s} is defined as the time when $\mathrm{d}E/\mathrm{d}\tau = 0$. Here, the disturbance thermal energy is defined as

$$E_1(\tau) = \int_0^1 \theta_1^2(z,\tau)\mathrm{d}z. \quad (21)$$

The strong stability limit may be relaxed by the relative stability criterion. Under the relative stability criterion, the relative instability time τ_{r} is determined as

$$r_1 = r_0 \text{ at } \tau = \tau_{\mathrm{r}}, \quad (22)$$

where the growth rates of r_1 and r_0 are defined as

$$r_1 = \frac{1}{E_1}\frac{\mathrm{d}E_1}{\mathrm{d}\tau} \text{ and } r_0 = \frac{1}{E_0}\frac{\mathrm{d}E_0}{\mathrm{d}\tau}. \quad (23a\&b)$$

Here E_0 is basic thermal energy, i.e. $E_0(\tau) = \int_0^1 \theta_0^2(z,\tau)\mathrm{d}z$ and using the basic temperature profile of Eq. (8), the growth rate of basic thermal energy r_0 can be obtained as

$$r_0 = \frac{\tau/3 - \sum_{n=1}^{\infty} 2/(n\pi)^4(1-\exp(-n^2\pi^2\tau))^2 - \sum_{n=1}^{\infty} 2\tau/(n\pi)^2(1-\exp(-n^2\pi^2\tau))}{\tau^2/3 + \sum_{n=1}^{\infty} 2/(n\pi)^6(1-\exp(-n^2\pi^2\tau))^2 - \sum_{n=1}^{\infty} 4\tau/(n\pi)^4(1-\exp(-n^2\pi^2\tau))}. \quad (24)$$

This relative stability criterion considers the temporal evolution of the basic and disturbance quantities. Taking the growth rate concept into account, the strong stability criterion corresponds to $r_1 = 0$ and for the limiting case of $\tau \to \infty$, the above growth rate reduced to $r_1 = 0$ and the relative stability degenerate into strong stability. The growth rate defined in Eq. (23a) is relatively insensitive to the number of terms used in Eq. (16). Therefore, the strong and relative stability criteria are adopted in the present work. Even the criteria of $E(\tau)/E(0) = 10^n$ $(n = 1,2,\ldots)$ was adopted as critical criteria [6] and predicted the experimental data quite well, these criteria do not have the deterministic meaning.

For the limiting case of $\tau \to 0$ it may be natural that $\theta_1(\tau,z) = \theta^*(\tau,\zeta)$ and $w_1(\tau,z) = w^*(\tau,\zeta)$, considering Eq. (9). We transform the disturbance equations such that the eigenfunctions associated with the diffusion operator are localized around the base-temperature front. Now, Eqs. (14) and (15) are transformed to the similarity variable of the base state, $\zeta = z/\sqrt{\tau}$. Then the perturbation equations can be expressed as

$$\left(\frac{\partial^2}{\partial\zeta^2} - a^{*2}\right)w_1^* = a^{*2}\theta_1^*, \quad (25)$$

$$\tau\frac{\partial\theta_1^*}{\partial\tau} - \left(\frac{\partial^2}{\partial\zeta^2} + \frac{\zeta}{2}\frac{\partial}{\partial\zeta} - a^{*2}\right)\theta_1^* = Ra_{\mathrm{D}}^* w_1^*\frac{\mathrm{d}\theta_0^*}{\mathrm{d}\zeta} \quad (26)$$

with the following boundary conditions,

$$w_1^* = \theta_1^* = 0 \text{ at } \zeta = 0 \text{ and } \zeta \to \infty. \quad (27)$$

Here $a^* = a\sqrt{\tau}$ and $Ra_{\mathrm{D}}^* = Ra_{\mathrm{D}}\tau^{3/2}$ are the wavenumber and the Darcy–Rayleigh number rescaled in the self-similar domain. By following Riaz et al. [3] procedure the streamwise operator of the temperature disturbance in the transformed coordinate, ζ, is expressed as

$$L = \frac{\partial^2}{\partial\zeta^2} + \frac{\zeta}{2}\frac{\partial}{\partial\zeta}, \quad (28)$$

and the temperature disturbance is expanded as

$$\theta_1^*(\tau,\zeta) = \sum_{k=1}^{\infty} A_k(\tau)\phi_k(\zeta) \quad (29)$$

with

$$L\phi_k = \lambda_k\phi_k(\zeta) = \lambda_k\exp(-\zeta^2/4)H_k(\zeta/2); \quad k = 0,1,2,\ldots \quad (30)$$

The eigenfunctions θ_k of L are the Hermite polynomials $H_k(\zeta/2)$ in the semi-infinite domain with weight function $\exp(-\zeta^2/4)$. The eigenvalues are $\lambda_k = -(k+1)/2$ for $k = 0,1,2,\ldots$ The most unstable eigenfunction, i.e. dominant mode solution satisfying the above boundary conditions (27) is given by

$$\phi_1 = \zeta\exp(-\zeta^2/4) \text{ and } L\phi_1 = -\phi_1(\zeta), \quad (31)$$

which are quite different from the conventionally used trial function [1,6], $(bz)^m\exp(-bz)$ where b is a scaling factor to improve the convergence. The first mode of the self-similar

diffusion operator decays with time while the rest of the spectrum decays more rapidly. Therefore the present analysis corresponds to the one term approximation with the most dangerous dominant mode solution.

By using the dominant mode solution, $\theta_1^* = A_1(\tau)\zeta\exp(-\zeta^2/4)$, substituting it into Eq. (25) and integrating across the domain, we obtain

$$\tau\frac{1}{A_1}\frac{dA_1}{d\tau} = -(1+a^{*2}) + Ra_D^*\left\langle \frac{w_1^*}{A_1}\frac{d\theta_0^*}{d\zeta}\right\rangle, \tag{32a}$$

where

$$\left\langle w_1^*\frac{d\theta_0^*}{d\zeta}\right\rangle = \frac{\int_0^\infty w_1^*\frac{d\theta_0^*}{d\zeta}d\zeta}{\int_0^\infty \zeta\exp(-\zeta^2/4)d\zeta}. \tag{32b}$$

By solving the following equation

$$\left(\frac{\partial^2}{\partial\zeta^2} - a^{*2}\right)\left(\frac{w_1^*}{A_1}\right) = a^{*2}\zeta\exp(-\zeta^2/4), \tag{33a}$$

$w^*(\tau,\zeta)$ can be obtained analytically as

$$\left(\frac{w_1^*}{A_1}\right) = \frac{a^*}{2}[\exp(a^*\zeta)\{f_1(\zeta) - f_1(\infty)\} - \exp(-a^*\zeta)\{f_2(\zeta) - f_1(\infty)\}] \tag{33b}$$

where

$$f_1(\zeta) = \int_0^\zeta \exp\left(-a^*x - \frac{x^2}{4}\right)xdx = \exp(a^{*2})\int_0^\zeta \exp\left\{-\left(a^* + \frac{x}{2}\right)^2\right\}xdx, \tag{33c}$$

and

$$f_2(\zeta) = \int_0^\zeta \exp\left(a^*x - \frac{x^2}{4}\right)xdx = \exp(-a^{*2})\int_0^\zeta \exp\left\{-\left(-a^* + \frac{x}{2}\right)^2\right\}xdx. \tag{33d}$$

The driving force for the instability, the integral $\left\langle w_1^*\frac{d\theta_0^*}{d\zeta}\right\rangle$, is also a function of time and the wavenumber.

From the relative stability condition of Eqs. (22) and (23) and the basic temperature distribution of Eq. (9) the following relation can be obtained:

$$r_1 = \frac{2}{A_1}\frac{dA_1}{d\tau} - \frac{\int_0^\infty \zeta\phi_1(d\phi_1/d\zeta)d\zeta}{\tau\int_0^\infty \phi_1^2 d\zeta} = \frac{5}{2\tau} = r_0 \quad \text{at } \tau = \tau_r. \tag{34}$$

After performing the integration in Eq. (34) using Eq. (31), at the relative stability condition the relation $(1/A_1)(dA_1/d\tau) = 1/\tau$ can be obtained and Eq. (32a) becomes

$$1 = -(1+a^{*2}) + Ra_D^*\left\langle \frac{w^*}{A_1}\frac{d\theta_0^*}{d\zeta}\right\rangle. \tag{35}$$

The strong stability condition of $dE/d\tau = 0$ means $(1/A_1)(dA_1/d\tau) = -1/(4\tau)$. Under the strong stability condition, Eq. (32a) reduces

$$-\frac{1}{4} = -(1+a^{*2}) + Ra_D^*\left\langle \frac{w^*}{A_1}\frac{d\theta_0^*}{d\zeta}\right\rangle. \tag{36}$$

The critical conditions can be determined analytically from Eqs. (35) and (36) when $\frac{\partial Ra_D^*}{\partial a^*} = 0$ with the critical wavenumber a_c^*.

3. Results and discussion

The primary concern of the initial value approaches is the effect of initial condition on the critical conditions. Even though the white noise employed in this study has been known as the fastest growing disturbance, the effect of the excitation time τ_e on the growth of disturbance has not been studied thoroughly. Here, the white noise is introduced at several times and its growth is summarized in Fig. 2. As shown in this figure, the effect of the excitation time on the disturbance growth is not predominant, i.e. the critical time is relatively insensitive to the excitation time. Therefore, in the present study, the white noise excited at $\tau = 0$ is employed as an initial condition.

The general feature of the numerical solution to the stability equation using the white noise initial conditions is described in Fig. 3. For a given wave number the disturbance initially slowly decays ($r_1 < 0$) until it reach the strong stability limit and the relative stability limit at which $r_1 = 0$ and $r_1 = r_0$, respectively. And then it grows superexponentially ($r_1 \gg r_0 > 0$). In Fig. 4, the strong and relative stability curves are given as a function of wave number. The minimum points of each curve constitute the strong and relative stability limit.

As the time tends toward infinity, the matrix I_{ml} is almost diagonal. Then the system of differential equations reduced as

$$\frac{dB_l}{d\tau} = \left[-\{(l\pi)^2 + a^2\} - 2Ra_D\frac{a^2}{(a^2+(l\pi)^2)}I_{ll}\right]B_l, \tag{37}$$

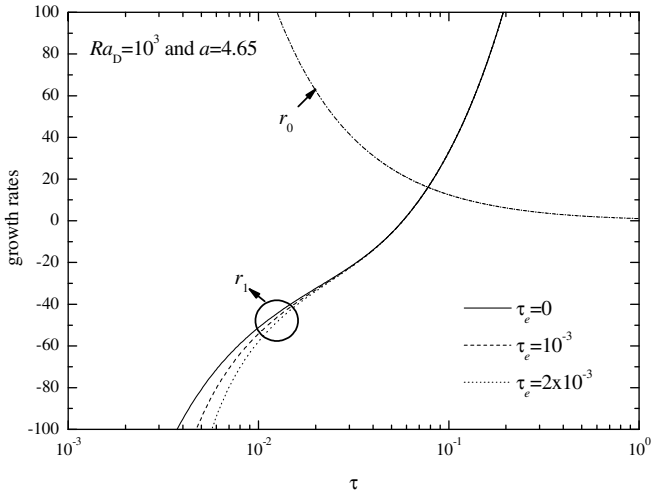

Fig. 2. Effect of excitation time τ_e on the growth rate of temperature disturbance.

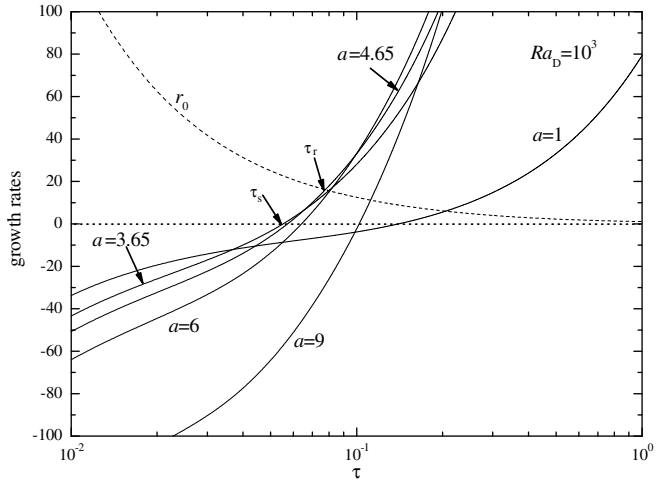

Fig. 3. Effect of wave number on the growth rate of temperature disturbance.

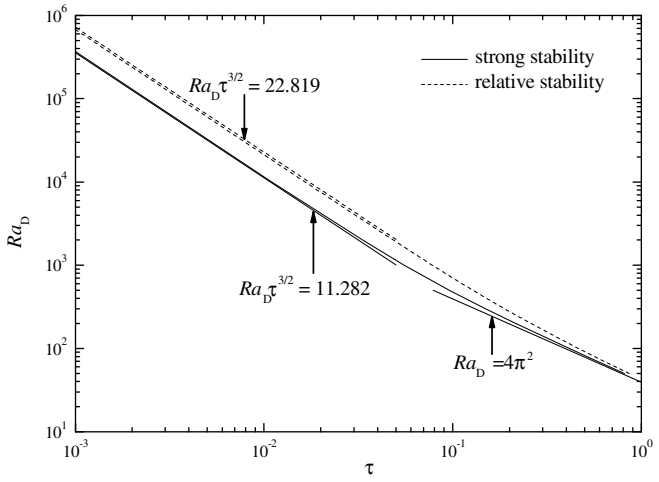

Fig. 5. Predicted critical times for a given Ra_D.

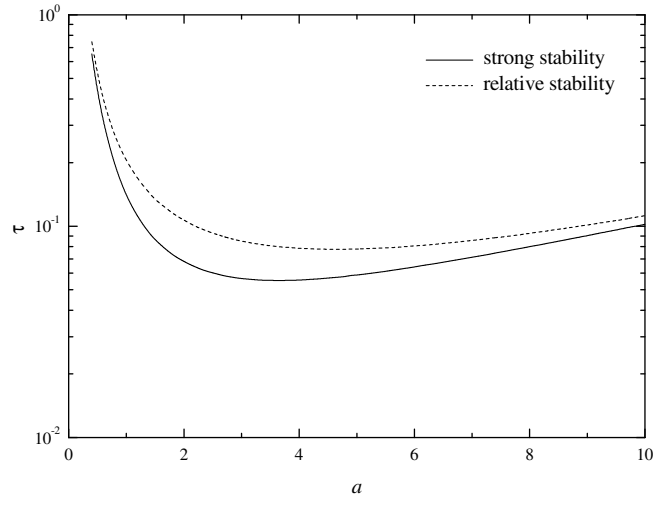

Fig. 4. Neutral stability curves for the critical times for the case of $Ra_D = 10^3$.

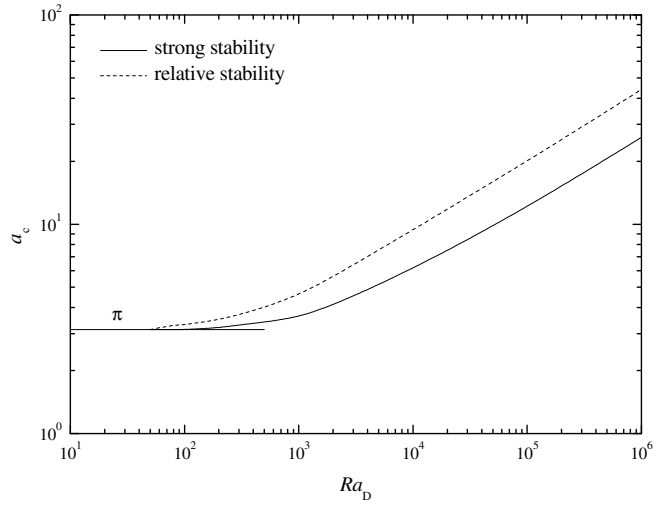

Fig. 6. Predicted wave numbers for a given Ra_D.

where $I_{ll} = \frac{\tau}{2} - \frac{1}{2\pi^2}\frac{\{1-\exp(-4l^2\pi^2\tau)\}}{4l^2}$. The critical time for the onset of convection can be deduced from Eq. (20) as

$$\{(l\pi)^2 + a^2\}^2 = Ra_D a^2\left\{\tau - \frac{\{1-\exp(-4l^2\pi^2\tau)\}}{4l^2}\right\} \quad \text{at } \tau = \tau_c. \tag{38}$$

As $\tau \to \infty$, the above result may be reduced as

$$Ra_D\tau \approx \frac{\{(l\pi)^2 + a^2\}^2}{a^2}. \tag{39}$$

Therefore, a minimum for the critical time is determined when

$$Ra_D\tau_c \approx 4\pi^2 \text{ at } a \approx \pi. \tag{40}$$

The strong and relative critical times are given as a function of Ra_D in Fig. 5. As shown in this figure the nominal critical times vary as $\tau_c \propto Ra_D^{-2/3}$ for $Ra_D \geqslant 10^3$. This means that the critical times are independent of the depth for large Ra_D. The variations of critical wavenumber as a function of Ra_D are given in Fig. 6. Here, it is found that the critical wave lengths are also independent of the depth for large Ra_D, i.e. $a_c \propto Ra_D^{1/3}$ for $Ra_D \geqslant 10^4$. And, as $\tau \to \infty$, the approximation of Eq. (40) gives the results that are close to the strong stability conditions. For the case of $Ra_D = 10^4$, the temporal evolution of temperature disturbance profiles is featured in Fig. 7. During the time period of $0 < \tau \leqslant 1.5\tau_r$, the temperature disturbance seems to modulate and finally to converge into a typical distribution. After this modulation period, the disturbance amplitude seems to keep growing with this spatial profile.

For the limiting case of $\tau \to 0$, with the dominant mode method, the marginal stability curve for the present absorption system of small time is given in Fig. 8 and the critical conditions are obtained as

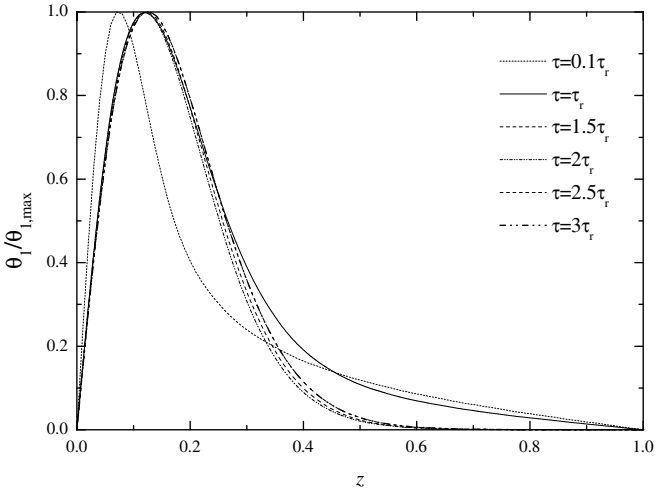

Fig. 7. Distribution of normalized temperature disturbance for a various time.

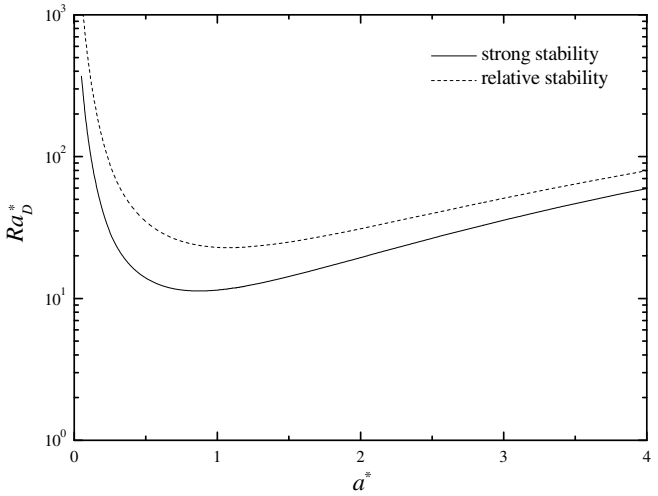

Fig. 8. Neutral stability curves for the limiting case of $\tau \to 0$.

$$Ra_D\tau_r^{3/2} = 22.819 \text{ and } a\sqrt{\tau_r} = 0 = 1.07, \tag{41}$$

$$Ra_D\tau_s^{3/2} = 11.282 \text{ and } a\sqrt{\tau_s} = 0 = 0.90. \tag{42}$$

These conditions are compared with the previous finite τ case in Fig. 5. Riaz et al. [3] claimed that this dominant mode method would yield exact results for small times but deviates from the exact solution for large times.

Foster [17] commented that with correct dimensional relations the relation of $\tau_0 \cong 4\tau_c$ would be kept for the case of horizontal fluid layers heated isothermally from below. This means that the growth period for disturbances to grow is required until they are detected experimentally. Therefore, it seems evident that the predicted onset time t_c is smaller than the detection time t_0. This means that a fastest growing mode of instabilities, which set in at $t = t_c$, will grow with time until manifest motion is first detected experimentally. If we choose τ_r as τ_c, the critical time can be expressed as

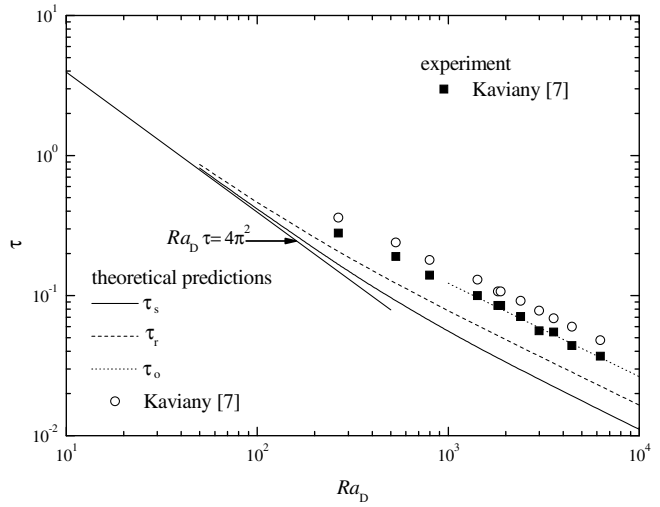

Fig. 9. Comparison of predicted critical time with the experimental data.

$$\tau_c = 7.72Ra_D^{-2/3} \quad \text{for } Ra_D \geqslant 10^3. \tag{43}$$

For the present system the Darcy–Rayleigh number based on the temperature difference is $Ra_D\tau$, so the critical condition of Eq. (43) is rearranged as

$$\tau_c = \left(\frac{21.43}{R_D}\right)^2 = 459R_D^{-2}, \tag{44}$$

where $R_D = Ra_D\tau$. From the Foster's comment ($\tau_0 \cong 4\tau_c$), the following relation can be obtained as

$$\tau_0 \cong 4\tau_c = 1836R_D^{-2}. \tag{45}$$

Since the temperature difference increase continuously during the growth period ($\tau_c \leqslant \tau \leqslant \tau_0$), the detection time τ_0 may be suggested as

$$\tau_0 = 1836(Ra_D\tau_0)^{-2}. \tag{46}$$

The present stability criteria compare well with Kaviany's [7] theoretical and experimental ones, as shown in Fig. 9. It is known that the relative stability limit, which is based on Eq. (46), is a good criterion to predict the critical time in the simple thermal systems.

4. Conclusion

The onset of buoyancy-driven motion in a fluid-saturated, horizontal porous layer heated from below with time-dependent manner has been analyzed analytically by using linear stability theory. The new stability criteria are introduced and analyzed by employing the initial value approach with the proper initial condition. The present stability criteria bound reasonably well extant experimental data. It seems that for deep-pool systems manifest convection is detected at t_0, considering experimental and theoretical results and for $\tau \leqslant \tau_0$ velocity disturbances are too weak to be observable experimentally. This means that convective motion will be detected experimentally at $\tau = 4\tau_r$. The present results show that the present stability

criteria can be applied to the stability analysis of the porous-saturated fluid systems.

References

[1] J. Ennis-King, I. Preston, L. Paterson, Onset of convection in anisotropic porous media subject to a rapid change in boundary conditions, Phys. Fluids 17 (2005) 084107.

[2] S.C. Hirata, B. Goyeau, D. Gobin, R.M. Cotta, Stability of natural convection in superposed fluid and porous layers using integral transforms, Numer. Heat Transfer, Part B: Fund. 50 (2006) 409–424.

[3] A. Riaz, M. Hesse, H.A. Tchelepi, F.M. Orr Jr., Onset of convection in a gravitationally unstable, diffusive boundary layer in porous media, J. Fluid Mech. 548 (2006) 87–111.

[4] C.W. Horton, F.T. Rogers, Convection currents in a porous medium, J. Appl. Phys. 6 (1945) 367–370.

[5] E.R. Lapwood, Convection of a fluid in a porous medium, Proc. Camb. Philos. Soc. 44 (1948) 508–521.

[6] T.D. Foster, Stability of homogeneous fluid cooled uniformly from above, Phys. Fluids 8 (1965) 1249–1257.

[7] M. Kaviany, Thermal convective instabilities in a porous medium, Trans. ASME: J. Heat Transfer 106 (1984) 137–142.

[8] G.M. Homsy, Global stability of time-dependent flows: impulsively heated or cooled fluid layers, J. Fluid Mech. 60 (1973) 129–139.

[9] P.C. Wankat, G.M. Homsy, Lower bounds for the onset time of instability in heated layers, Phys. Fluids 20 (1977) 1200–1201.

[10] J.-P. Caltagirone, Stability of a saturated porous layer subject to a sudden rise in surface temperature: comparison between the linear and energy methods, Quart. J. Mech. Appl. Math. 33 (1980) 47–58.

[11] M.C. Kim, H.K. Park, C.K. Choi, Stability of an initially, stably stratified fluid subjected to a step change in temperature, Theor. Computat. Fluid Dyn. 16 (2002) 49–57.

[12] M.C. Kim, S. Kim, B.J. Chung, C.K. Choi, The onset of convective instability in a horizontal porous layer saturated with oil and a layer of gas underlying it, Int. Commun. Heat Mass Transfer 20 (2003) 225–234.

[13] K.K. Tan, R.B. Thorpe, The onset of convection caused by buoyancy during transient heat conduction in deep fluids, Chem. Eng. Sci. 51 (1996) 4127–4136.

[14] K.-K. Tan, T. Sam, H. Jamaludin, The onset of transient convection in bottom heated porous media, Int. J. Heat Mass Transfer 46 (2003) 2857–2873.

[15] Y. Katto, T. Masuoka, Criterion for onset of convection in porous medium, Int. J. Heat Mass Transfer 10 (1967) 297–309.

[16] S. Chandrasekhar, Hydrodynamic and Hydromagnetic Stability, Oxford University Press, London, 1961.

[17] T.D. Foster, Onset of manifest convection in a layer of fluid with a time-dependent surface temperature, Phys. Fluids 12 (1969) 2482–2487.